Materials Research Proceedings 46 (2024) 41-48 https://doi.org/10.21741/9781644903377-6

Addressing surface quality via seam alignment parametrization

Alexandru-Ionuț IRIMIA[1, a, *], Vasile ERMOLAI[1, b], Gheorghe NAGÎȚ[1, c], Marius-Andrei MIHALACHE[1, d], Marius-Ionuț RÎPANU[1, e], Răzvan-Cosmin STAVARACHE[1, f]

[1]"Gheorghe Asachi" Technical University of Iași, Department of Machine Manufacturing Technology, Blvd. Dimitrie Mangeron 59A, Iași, 700050, Romania

[a]alexandru-ionut.irimia@student.tuiasi.ro, [b]vasile.ermolai@academic.tuiasi.ro, [c]gheorghe.nagit@academic.tuiasi.ro, [d]marius-andrei.mihalache@academic.tuiasi.ro, [e]marius-ionut.ripanu@academic.tuiasi.ro, [f]razvan-cosmin.stavarache@student.tuiasi.ro

Keywords: Fused Filament Fabrication, Surface Quality, Surface Finish, Z-Seam, Seam Alignment

Abstract: Fused Filament Fabrication (FFF) is an additive manufacturing technology that uses molten thermoplastic material to build parts layer-wise. Any of the part's constituent layers is obtained through multiple passes of the extrusion heat. An external contour or perimeter and an internal geometry characterize each layer. This external contour is defined by a start-point, an extrusion path, and an end-point, which coincides with the starting point. The overlap between the extrusion path's start and the end-point is known as z-seam alignment or seam. By default, the slicing algorithms place the seams at sharp corners or hidden edges to hide possible imperfections such as blobs and zits. Unfortunately, seam hiding is more difficult for curved surfaces without linear transitions. As a result, the curved surface printed parts show visible seams of the external contour, affecting the part's aesthetics. In this regard, this study aims to reduce some of those limitations by systematically fine-tuning the seam-related parameters.

Introduction

Fused Filament Fabrication (FFF) is an additive manufacturing process that builds parts through the selective deposition of semi-molten materials in filaments with rectangular-like cross-sections [1].

Due to low-cost equipment, relatively good quality and mechanical properties, and great availability of raw materials at a fraction of cost compared to other additive technologies (e.g., SLS) FFF has become one of the most known additive manufacturing (AM) techniques [2]. Other benefits of FFF, and other AM technologies, are the complexity for free (i.e., the manufacturing cost is not affected by the part’s complexity) and the reduced material waste compared to conventional manufacturing (e.g., turning, milling) [3].

As for any manufacturing process, the part’s resulting quality is influenced by multiple variables such as equipment precession, process variables, material properties, or environment specifics [4-6].

In the case of FFF, the seam-related parameters are a specific category of parameters, met only for extrusion-based AM technologies. FFF builds parts from multiple elements: shells, internal structures, and solid layers. The seam is located on the part’s shells, as any shell profile is characterized by a start and end-point [7, 8]. Harum et al. observed that seams become visible as the excess material is squeezed out at the closing point resulting in a poor surface finish [9]. The literature review shows that seam effects were discussed due to their effect on the surface quality. However, none of these studies documented and studied the effect of seam parameters on surface quality. This study aims to document and study the effect of seam parameters on the resulting

surface quality. The chosen variables are directly influencing resulting seams visibility on parts' outer surfaces.

Seam parameters

As stated above, a seam represents the location where the start and the endpoint of a shell or wall intersect. Frequently the slicing algorithm chooses the seam location based on the layer's profile (e.g., ellipse, hexagon) and the slicing algorithm inputs (which will be further discussed below). As a rule of thumb, the seam is placed at the sharpest corner for polygonal profiles, while for curved profiles it will be placed at a random location if not specified [7-9].

The illustration presented in Fig. 1 was designed to better understand how seams are placed based on the profile. Both profiles, round (Fig. 1a) and squared (Fig. 1b) show a front seam positioning. As seen, for the round profile the seam is placed at the specific location. However, for the squared profile, the seam is located in the same plane but on the corner. In the Ultimaker Cura slicing software the seam position is controlled through the *Z Seam Alignment* parameter. The variable has multiple seam positioning options, as follows: *User Specified*, *Shortest*, *Random,* and *Sharpest Corner* [7, 8]. The illustration below simulates a *User Specified*, in this case, *Front*, *Z Seam Alignment*.

The *Seam Corner Preference* extends the above-described variable and controls how the seam will be positioned relative to the model. The variable controls how the hidden or exposed seam will be placed based on the following parametrization levels: *None, Hide Seam, Expose Seam, Hide or Expose Seam,* and *Smart Hiding* [7, 8].

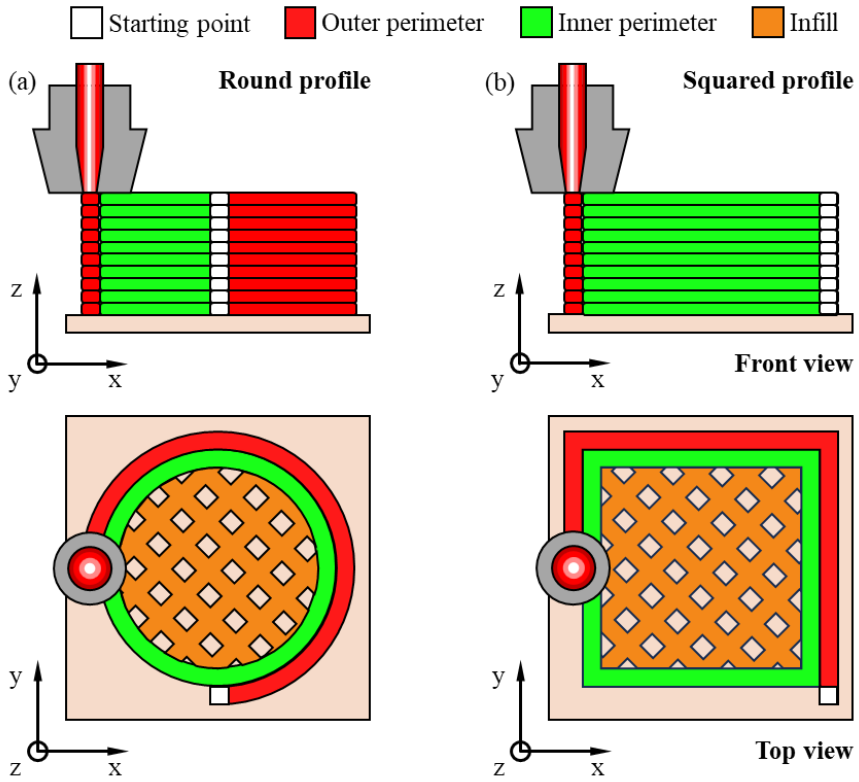

Fig. 1. Seam formation (a) circular profile vs (b) rectangular profile.

Besides the seam relative position control, the Cura slicer provides alternative ways to reduce the seam visibility on the outer surface through the *Outer Wall Wipe Distance* and *Coasting Volume* [7, 8].

In Cura, the *Outer Wall Wipe Distance* variable can be found in the Walls tab together with the previous two. This parameter makes the extrusion head to crossover the contour endpoint without extruding. The crossover distance is set by the user (see the dark red colored zone from Fig. 2b) and allows the printer to wipe out the nozzle against the outer wall. This way, any extra amount of molten material or over-extrusion is evenly spread across the wipe distance before going on to the next layer. This parameter becomes very useful to prevent molten material from oozing before the material filament is retracted out of the heated zone. Setting the *Outer Wall Wipe Distance* too high can lead to under-extrusion, as the molten material reservoir empties too much. Basically, in the time frame needed to switch layers and begin a new one, there is not enough time for the feeding mechanism to replenish the melt reservoir [7, 8]. This scenario can be limited by firstly printing the internal structure and by choosing an inside-to-outside wall ordering [10].

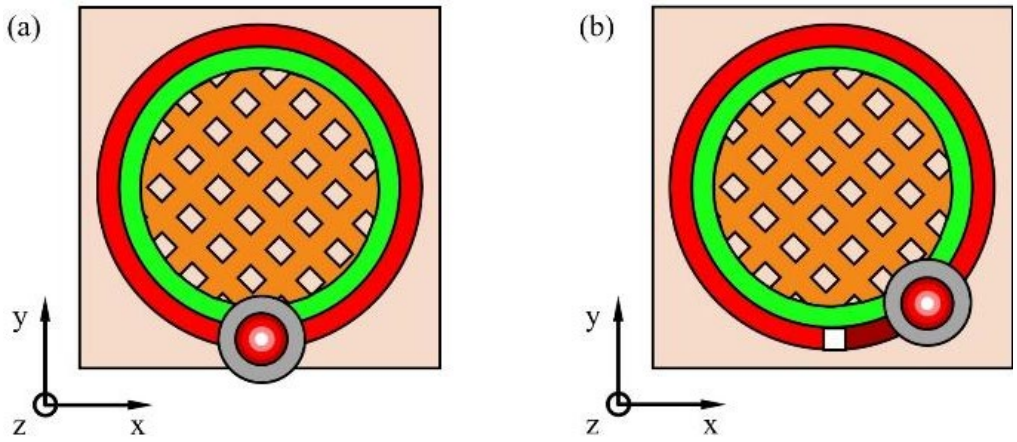

Fig. 2. Outer wall wipe distance (a) with wipe, (b) without wipe.

The *Coasting Volume* parameter can be found in the Experimental tab of the same slicing tool. This variable makes the feeding mechanism stop extruding the filament before the nozzle meets the outer contour endpoint by setting the coasting volume [7, 8, 11]. In other words, for a certain length, the nozzle will follow the deposition path without extruding as illustrated in Fig. 3.b. In a way, the use of *Coasting Volume* can be considered a pre-retraction step. Similarly to the *Outer Wall Wipe Distance*, it compensates for blobs and exposed seams formation. However, over-increasing the *Coasting Volume* can lead to under-extrusion in the seams area [7, 8]. This effect could be further amplified if combined with a null wipe distance.

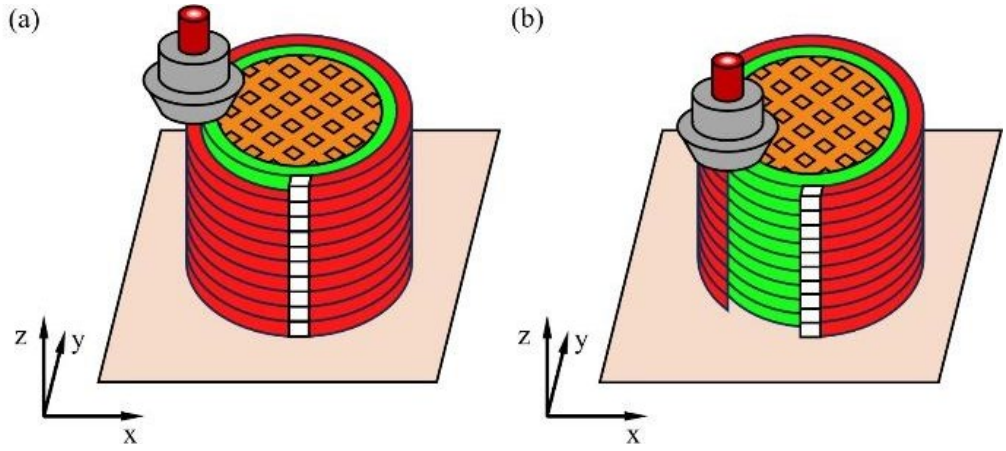

Fig. 3. Coasting Volume - (a) coasting activated, (b) coasting deactivated.

Design of experiment

The experimental research was made based on L9 (3^4) Taguchi experimental design [12-14] with four factors on three levels of variation. The chosen factors are the above-described variables, namely: *Z Seam Alignment (ZSA), Seam Corner Preference (SCP), Outer Wall Wipe Distance (WD),* and *Coasting Volume (CV)*.

Based on the information shown in the previous section, it can be stated that the ZSA and SCP variables' levels of variation exceed the Taguchi L9 design matrix. However, this orthogonal matrix with the chosen levels of variation gives the highest level of variability. When simulating other Taguchi designs (i.e., L16 and L18) it was observed that some variable levels make other factor levels unavailable. This way, the L9 matrix had the highest factor variation availability.

For the chosen factor the variation levels were used as follows:

- ZSA: User Specified (US), Shortest (S) and Sharpest Corner (SC);
- SCP: None (N), Hide Seam (HS) and Expose Seam (ES);
- WD: 0, 0.2 and 0.4 mm;
- CV: 0, 0.03 and 0.06 mm^3.

According to the L9 design matrix, nine determinations were performed in total, which respect the parametrization described in Table 1.

Table 1. Experimental design Taguchi.

Run no.	ZSA	SCP	WD	CV
R1	US	N	0	0
R2	US	HS	0.2	0.03
R3	US	ES	0.4	0.06
R4	S	N	0.2	0.06
R5	S	HS	0.4	0
R6	S	ES	0	0.03
R7	SC	N	0.4	0.03
R8	SC	HS	0	0.06
R9	SC	ES	0.2	0

The influence of the above-described variables was evaluated based on the resulting seam area for custom conical specimens with a 40° incline refeed to the XY base plane. All specimens were printed on an Ultimaker 2+ only with two shells using a Fillamentum PLA Ivory material.

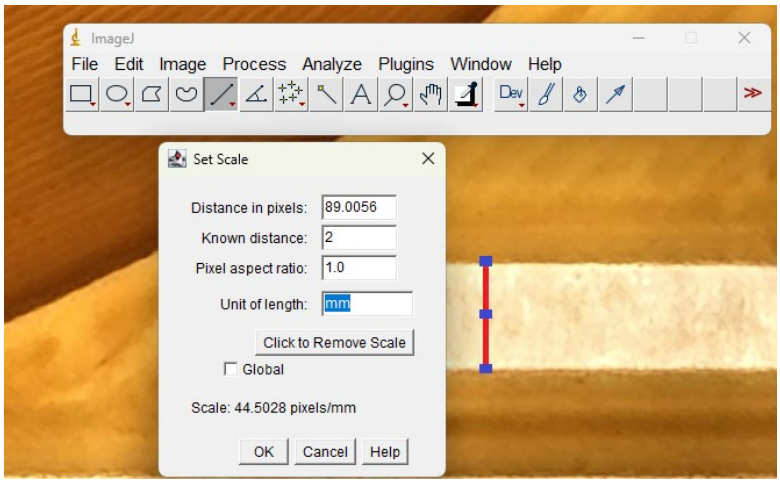

Fig. 4. Set scale to a known dimension.

The seam area was measured through visual inspection. This way, each sample was photographed and the resulting image was further analyzed using the ImageJ [15, 16]. To ensure precise measurements, ImageJ needs a reference scale. This way each of the nine samples was designed with a predefined L-shaped scale having a 2 mm gap as a reference. First, the gap was measured using a Mitutoyo caliper. Then the ImageJ measurement tool was used to set the right scale, as shown in Fig. 4.

Results

For each resulting sample, the seam area was measured using ImageJ. This was achieved by using a lasso function available in the software's analyze menu. A preview of the described methodology is presented below in Fig. 5.

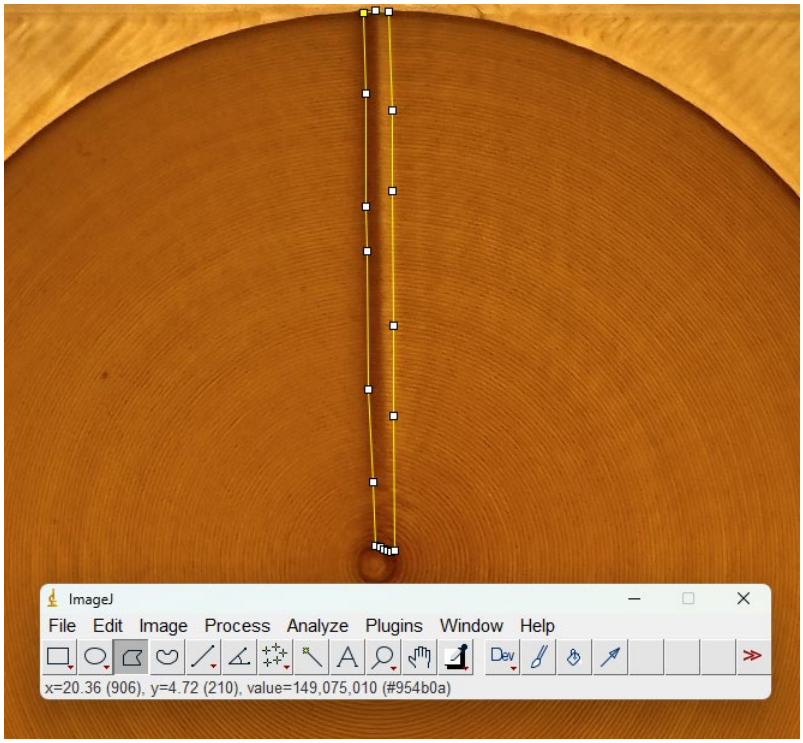

Fig. 5. Sample area measurement using ImageJ.

Since the seam area is selected by the ImageJ software's user, for the same measured seam, either by the same user or by a different one, the area value will never be identical to another determination. This happens because there is a small probability of picking the same measuring point consecutively. This way, each feature needs to be measured multiple times. The area values shown in Table 2 are the averages of five determinations. The provided results have a relatively small deviation of 0.457-1.507 mm^2.

Table 2. Seam area value resulted.

Run no.	R1	R2	R3	R4	R5	R6	R7	R8	R9
Resulting area (mm^2)	42.35	50.06	49.67	46.32	44.34	46.02	48.91	52.86	40.73
	46.43	51.09	49.15	46.70	43.87	44.02	49.20	50.77	41.64
	43.68	51.65	49.40	47.75	43.59	44.61	48.42	51.35	40.83
	44.67	51.17	49.91	46.16	42.21	45.20	47.92	51.48	40.36
	44.83	52.91	50.33	46.09	43.03	44.66	49.67	51.80	40.56

Average	44.39	51.38	49.69	46.60	43.41	44.90	48.82	51.65	40.82
St. dev.	1.507	1.036	0.457	0.683	0.820	0.752	0.678	0.773	0.490

The factors' variations show that, when the ZSA is used with the level *Shortes* (i.e., print head shortest travel movement relative to the absolute coordinate system), the seam orientation angle is offset by 135° in a clockwise direction as shown in Fig. 6. At first view, the *Seam Corner Preference* variable could be responsible for the R4, R5, and R6 seam offset. However, there is not enough evidence to indicate that for the Sharpesr Corner ZSA, the resulting seam will always have the location presented in Fig. 6 (i.e., R4, R5, and R6).

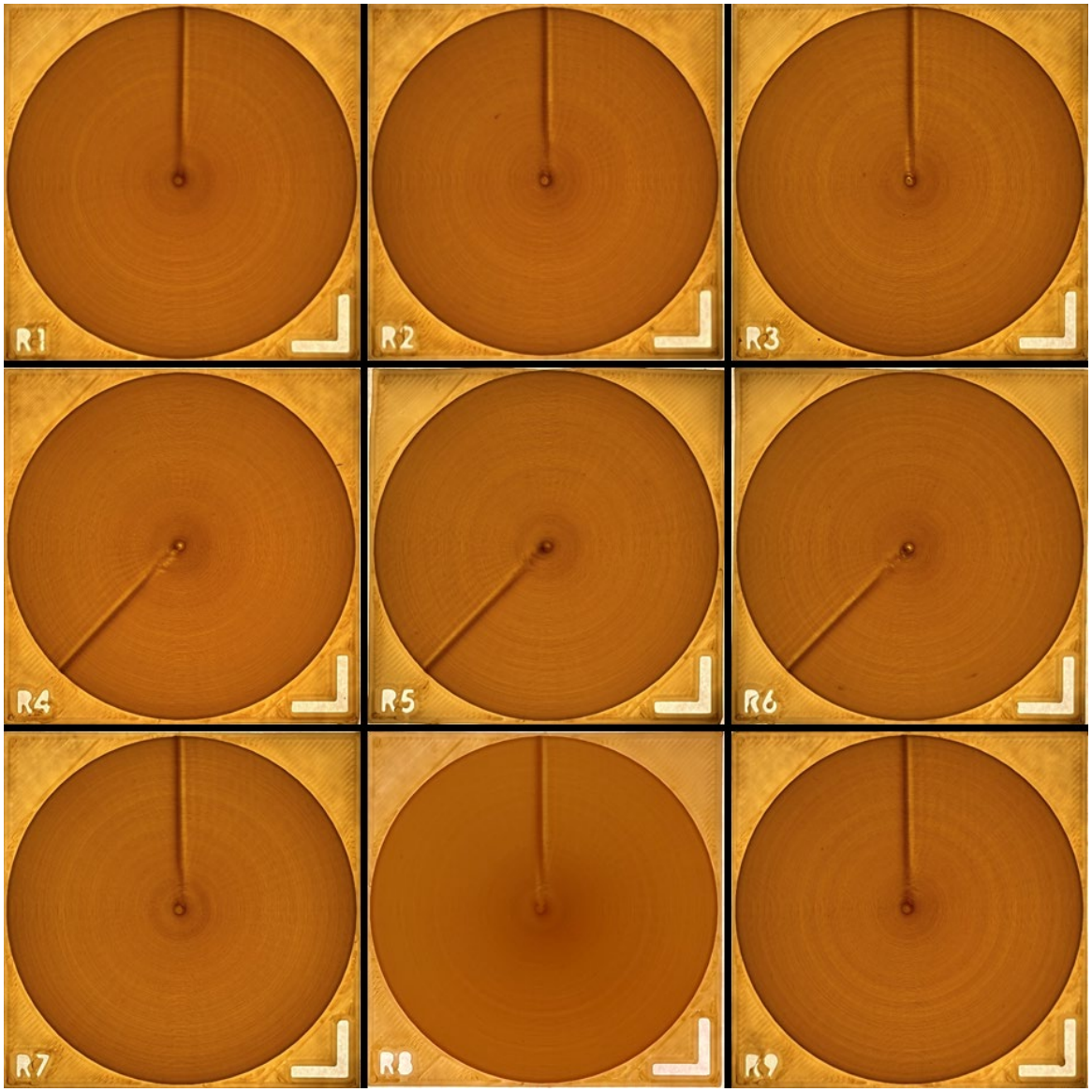

Fig. 6. Image of the Taguchi L9 resulting samples.

The resulting seam area measurements presented in Table 2 were plotted using bar charts as shown in Fig. 7. From this, results that the R9 variables' configuration provides the smallest seam area, having 40.82±0.49 mm^2. However, when judging based on aesthetics the R8 variable configuration shows better results, even if the resulting seam area is the highest.

The data provided in Table 2 and Fig.7 shows that the measured seam area varied between 43.4±0.457 mm^2 (i.e., R3) and 51.65±0.773 mm^2 (i.e., R8) with the highest standard deviation of 1.507 mm^2 (i.e., R1).

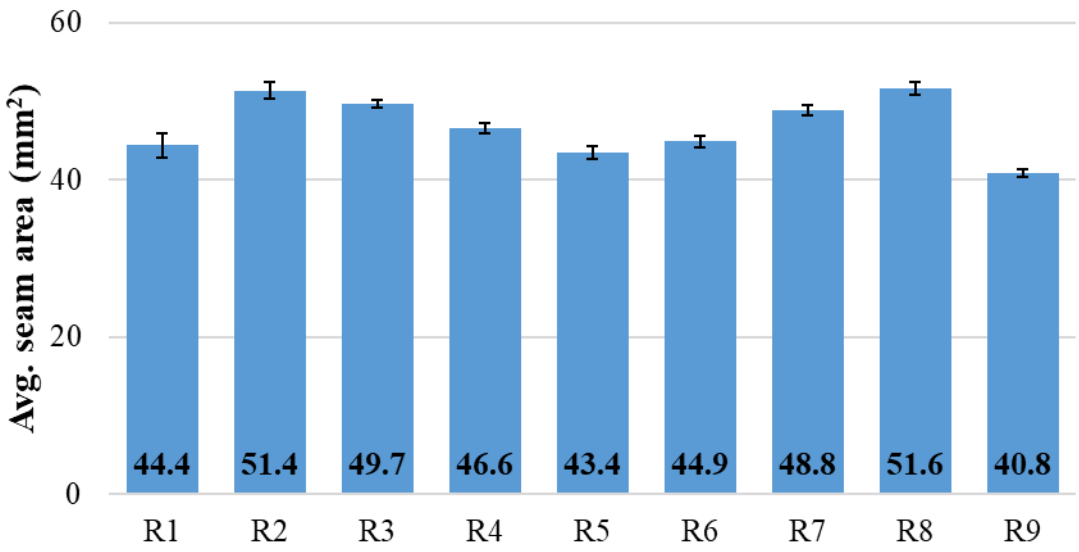

Fig. 7. Bar plot of the resulting seam area.

Conclusions

In Fused Filament Fabrication, several factors influence the seam characteristics of a part's outer surface. These factors include Z *Seam Alignment, Seam Corner Preference, Outer Wall Wipe Distance*, and *Coasting Volume*. While smaller seam areas are generally preferred for reducing exposed material on the part's surface, they don't always offer the best aesthetics. In this case, the R8 parameter configuration delivered the best outer surface quality, even though it resulted in the largest seam area.

The seam parametrization data for FFF 3D-printed parts highlight the trade-off between seam area exposure and aesthetic. Achieving a balance between the part's structural integrity and visual quality is desirable.

Future work can focus on further optimizing these variable configurations and exploring new ones, such as extrusion temperature and alternative filament materials. This approach may provide more insights into seam parametrization, helping improve seam outlook without compromising the part's strength.

References

[1] J. Kechagias, D. Chaidas, N. Vidakis, K. Salonitis, N.M. Vaxevanidis, Key parameters controlling surface quality and dimensional accuracy: a critical review of FFF process. Mater. Manuf. Proces., 37(9), 963-984 (2022). https://doi.org/10.1080/10426914.2022.2032144

[2] Krishnanand, M. Taufik, Fused filament fabrication (FFF) based 3D printer and its design: a review. Advanced Manufacturing Systems and Innovative Product Design: Select Proceedings of IPDIMS 2020, 497-505 (2021). https://doi.org/10.1007/978-981-15-9853-1_41

[3] R. B. Kristiawan, F. Imaduddin, D. Ariawan, Ubaidillah, Z. Arifin, A review on the fused deposition modeling (FDM) 3D printing: Filament processing, materials, and printing parameters. Open Engineering, 11(1), 639-649 (2021). https://doi.org/10.1515/eng-2021-0063

[4] R. Patel, C. Desai, S. Kushwah, M.H. Mangrola, A review article on FDM process parameters in 3D printing for composite materials. Materials Today: Proceedings, 60, 2162-2166 (2022). https://doi.org/10.1016/j.matpr.2022.02.385

[5] S. Restrepo, J. Jaramillo, H.A. Colorado, Fused Filament Fabrication (FFF) Additive manufacturing of Bronze-Based materials. In The Minerals, Metals & Materials Series, 105–112 (2024). https://doi.org/10.1007/978-3-031-50349-8_10

[6] V. Ermolai, A. Sover, G. Nagîț, M. A. Boca, A.I. Irimia, Influence of Fused Filament Fabrication Raster Parameters over the Top Surface Topography. Acta Technica Napocensis-Series: Applied Mathematics, Mechanics, And Engineering, 66(5) (2023).

[7] UltiMaker. (2024, August 30). UltiMaker Cura - UltiMaker. https://ultimaker.com/software/ultimaker-cura/

[8] Ghostkeeper. (n.d.). GitHub - Ghostkeeper/SettingsGuide: More extensive explanations of Cura slicing settings. GitHub. https://github.com/Ghostkeeper/SettingsGuide

[9] V. Ermolai, A. Sover, (2023). Multi-material 3D Printed Interfaces. Influencing Factors and Design Considerations. In: Cioboată, D.D. (eds) International Conference on Reliable Systems Engineering (ICoRSE) - 2023. ICoRSE 2023. Lecture Notes in Networks and Systems, vol 762. Springer, Cham. https://doi.org/10.1007/978-3-031-40628-7_11

[10] N. Harun, N. Kasim, M. Abidin, M. Izamshah, R. Attan, H. Ganesan., A Study on Surface Roughness During Fused Deposition Modelling: A Review. JAMT, 12(1(1), 25-36 (2018).

[11] V. Ermolai, A. Sover, A. Lang, Characterisation of the shape memory effect of PET polymer by FFF 3D printing. MRP, 28 (2023). https://doi.org/10.21741/9781644902479-11

[12] S. K. Karna, R. Sahai, An overview on Taguchi method. International journal of engineering and mathematical sciences, 1(1), 1-7 (2012).

[13] A. Freddi, M. Salmon, A. Freddi, M. Salmon, Introduction to the Taguchi method. Design principles and methodologies: from conceptualization to first prototyping with examples and case studies, 159-180 (2019). https://doi.org/10.1007/978-3-319-95342-7_7

[14] A. Mitra, The Taguchi method. Wiley Interdisciplinary Reviews: Computational Statistics, 3(5), 472-480 (2011). https://doi.org/10.1002/wics.169

[15] ImageJ. (n.d.). https://imagej.net/ij/

[16] T. (n.d.) Ferreira, ImageJ User Guide - IJ 1.46R. https://imagej.net/ij/docs/guide/index.html